Spatiotemporal Intermittency in Rayleigh-Bénard Convection

S. Ciliberto and P. Bigazzi
Istituto Nazionale Ottica, 6-50125 Firenze, Italy
(Received 13 October 1987)

The transition to spatiotemporal intermittency has been experimentally studied in Rayleigh-Bénard convection in an annular cell. The dynamics of the system has been analyzed by computation of the statistical distribution of turbulent and laminar regions. The results, which display features typical of phase transitions, are similar to those found in systems of coupled maps and in partial differential equations.

PACS numbers: 47.25.Qv, 05.70.Jk

The transition to spatiotemporal chaos is a problem of great current interest that has been theoretically studied in systems of coupled maps[1] and in partial differential equations (PDE).[2,3] One of the typical chaotic regimes presented by these two mathematical models is spatiotemporal intermittency. It consists of a fluctuating mixture of laminar and turbulent domains with well-defined boundaries.[2] Such a behavior appears also in some cellular automata.[4]

Qualitative experimental observations of this phenomenon in Rayleigh-Bénard convection[5] and in boundary-layer flows[6] have been reported; however, to the best of our knowledge, no quantitative characterization is available. We report here a statistical analysis of the onset of spatiotemporal intermittency done in an experiment on Rayleigh-Bénard convection. Our results, which display features typical of phase transitions, are similar to those recently obtained by Chaté and Manneville in numerical simulations of a PDE[2] and by Kaneko in systems of coupled maps.[1a]

The system of interest is an annular fluid layer confined between two horizontal plates and heated from below. When the temperature difference ΔT exceeds the threshold value ΔTc a steady convective flow consisting of radial rolls (roll axes along radial directions) arises. With the annular geometry the spatial pattern has periodic boundary conditions. Furthermore, the sizes of our cell constrain the convective structure to an almost one-dimensional chain of rolls.

The inner and outer diameters of the annulus are 6 and 8 cm, respectively, and the depth of the layer is 1 cm. The lateral walls are made of Plexiglas, while the bottom and top plates are respectively made of copper and sapphire. The upper plate, which allows for optical inspection, is cooled on its top by a circulation of water whose temperature is stabilized by a thermal bath. The copper plate, which has its upper surface polished and covered by a nickel film, is heated by an electronic circuit that stabilizes ΔT. The cell is enclosed in a stabilized temperature box. The stability of ΔT is about ± 1 mdeg C. The working fluid is silicone oil with a Prandtl number of about 30. The critical value of ΔT at the onset of convection is $\Delta T_c = 0.06\,°\mathrm{C}$.

For quantitative analysis, we use a technique based on the measurement of the deflections of a laser beam that sweeps the fluid layer. The principle of the method has already been described elsewhere[7] and applied to the study of the convective motion.[8] The actual setup provides the possibility of measuring, with a twelve-bit resolution, the two components of the thermal gradient $\{(1/r)[\partial T(r,\theta,t)/\partial\theta], \partial T(r,\theta,t)/\partial r\}$ averaged along the vertical direction, in the polar coordinate reference frame r,θ. The accuracy of the measurement is about 7%, the sensitivity 0.01 °C/cm, and the spatial resolution about 1 mm.

The space-time evolution of the system has been characterized by use of $u(\theta,t) = (1/r_0)[\partial T(r_0,\theta,t)/\partial\theta]$, that is the component of the temperature gradient perpendicular to the roll axis. The function $u(x,t)$, where $x = \theta/2\pi$, is sampled at 128 points in space on the circle of radius $r_0 = 3.6$ cm. When the regimes are time dependent $u(x,t)$ is recorded for at least 5000 times at intervals of 1 sec, that is about $\frac{1}{10}$ of the main oscillation period of our system.

Analyzing the fluid behavior as a function of $\eta = \Delta T/\Delta T_c$, we observe that, for η around 1, the spatial structure has 24 rolls. This number increases with η and reaches 38 at η around 200.[9] The spatial structure remains stationary for $\eta < 183$ where a subcritical bifurcation to the time-dependent regime takes place. For $\eta \geq 183$, the time evolution is chaotic but, if we reduce η, the system presents either periodic or quasiperiodic oscillations, and at $\eta = 152$ it is again stationary. In the range $152 < \eta < 200$ the time dependence consists of rather localized fluctuations that slightly modulate the convective structure, which maintains its periodicity. The detailed analysis of this behavior will be reported elsewhere.

The regime to be described in this Letter begins at $\eta = 200$. A typical example of the space-time evolution of $u(x,t)$ in this regime at $\eta = 248$ is reported in Fig. 1. It presents at the same time several domains where the spatial periodicity is completely lost (we will refer to them as turbulent) and other regions (that we call laminar) where the spatial coherence is still maintained. In the turbulent domains the time evolution is characterized

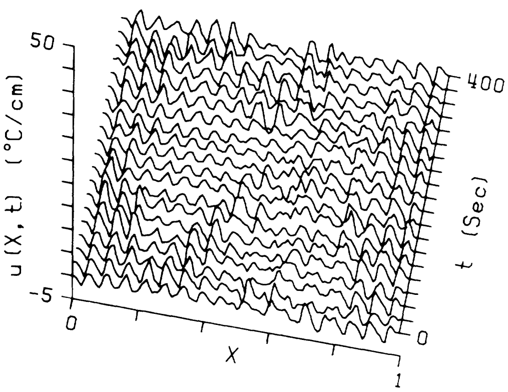

FIG. 1. Space-time evolution of $u(x,t)$ at $n = 248$.

by the appearance of large oscillatory bursts that locally destroy the spatial order. Instead in laminar regions the oscillations remain very weak.

Thus the two regions can be identified by measurement of the local peak-to-peak amplitude for a time interval comparable with the mean period of the oscillation.[10] Choosing a cutoff α, and making black all the points where the oscillation amplitude is above α, we can easily represent the dynamics of turbulent and laminar regions. As an example of such a code we show the space-time evolution of $u(x,t)$ at $\eta = 216$ in Fig. 2(a), and $\eta = 248$ in Fig. 2(b). We remark that the qualitative features of these pictures are rather independent of the precise value of the cutoff.

At $\eta = 216$ [Fig. 2(a)], a wide laminar region surrounds completely the turbulent patches that remain localized in space, after their appearance. Furthermore, the nucleation of a turbulent domain has no relationship with the relaxation of another one. In contrast, at $\eta = 248$ [Fig. 2(b)], the turbulent regions migrate and

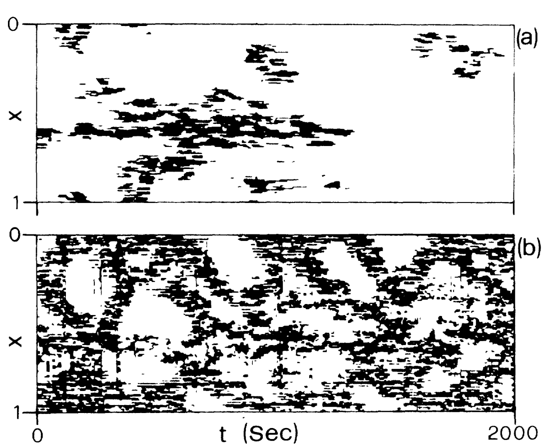

FIG. 2. Binary representation, at $\alpha = 1.5\,°\mathrm{C/cm}$, of the space-time evolution of $u(x,t)$ at (a) $\eta = 216$ and (b) $\eta = 248$. The dark and white areas correspond to turbulent and laminar domains, respectively.

slowly invade the laminar ones. This regime, that sets in for $\eta > 245$, will be called spatiotemporal intermittency because of the remarkable analogy of Fig. 2(b) with those obtained in systems of coupled maps that present such a behavior.[1a]

Furthermore, we notice that the change from the regime of Fig. 2(a) to that of Fig. 2(b) is reminiscent of a percolation,[11] that, indeed, has been proposed as one of the possible mechanisms for the transition to spatiotemporal intermittency.[2,12] The two qualitative analogies, with coupled maps and percolation, suggest that in our system the transition to the regime reported in Fig. 2(b) may present itself as a phase transition, occurring for $245 < \eta < 248$.

Following the method used by Kaneko[1a] and Chaté and Manneville,[2] we quantitatively characterize such a behavior by computing, over a time interval of 10^4 sec, the distribution $P(x)$ of the laminar domains of length x. The existence of two different regimes is clearly shown in Figs. 3(a) and 3(b) which display $P(x)$ versus x at $\eta = 241$ and $\eta = 310$, respectively. At $\eta = 241$, Fig. 3(a), $P(x)$ decays with a power law. The exponent, equal to 1.9 in Fig. 3(a), does not depend, within our accuracy, either on α or on n. Its average value is $\mu = 1.9 \pm 0.1$.

On the other hand, at $\eta = 310$, Fig. 3(b), the decay for $x > 0.1$ is exponential with a characteristic length $1/m = 0.10$. The dependence of m on α is the following:

$$m(\alpha,\eta) = m_0(\eta)\exp(-\alpha/\alpha_0), \tag{1}$$

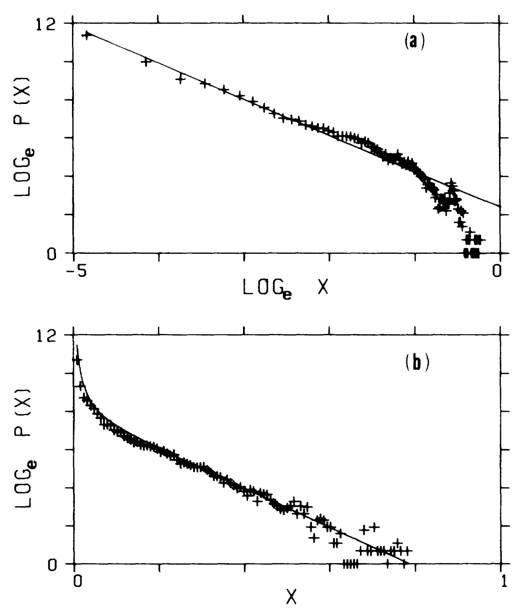

FIG. 3. Distribution $P(x)$ of the laminar domains of length x. (a) $\eta = 241$, the algebraic decay with exponent 1.9; (b) $\eta = 310$, and $\alpha = 1.6\,°\mathrm{C/cm}$, exponential decay with a characteristic length $1/m = 0.10$. The solid lines are obtained from Eq. (3).

with $\alpha_0 = (0.87 \pm 0.06)\,^\circ\mathrm{C/cm}$, independent of η. The values of m versus α at $\eta = 310$ and $\eta = 262$ are reported in Fig. 4(a) on a semilogarithmic scale. For $\alpha < 0.4\,^\circ\mathrm{C/cm}$ there are no experimental points because at very small α the following problems arise: (i) The amplitudes of weak laminar oscillations are above the cutoff, and therefore our method is not able to discriminate between turbulent and laminar domains; (ii) very long time series are needed to have reliable statistics because the probability of finding laminar regions decreases on reduction of the cutoff; (iii) the measurements are affected by the experimental noise. By doing a linear best fit of the experimental points for $\alpha > 0.4\,^\circ\mathrm{C/cm}$ we can extrapolate the measurement to $\alpha = 0$ thus obtaining $m_0(\eta)$. The dependence of $m_0^2(\eta)$ as a function of η is reported in Fig. 4(b). The linear best fit for $\eta > 246$ of the points of Fig. 4(b) gives the following result:

$$m_0(\eta) = m_1(\eta/\eta_s - 1)^{1/2}, \tag{2}$$

with $\eta_s = 247 \pm 1$ and $m_1 = 117 \pm 2$. This equation shows the existence of a well-defined threshold η_s for the appearance of an exponential decay in $P(x)$. Besides, we see that the characteristic length $1/m_0$ diverges at $\eta = \eta_s$. However, for $\eta \leq 247$, we find that the minimum of m_0 is of the order 1 as it should be expected because $1/m_0$ cannot be bigger than the size of the system.[13] Indeed the curvature for $\ln x > -1$, in Fig. 3(a), is related to this finite-size effect.

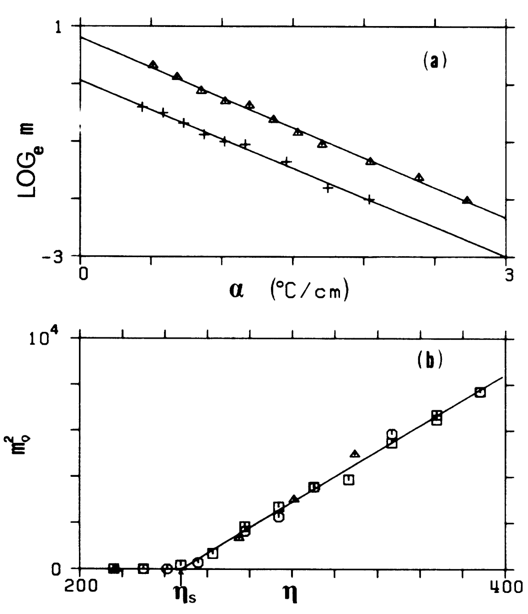

FIG. 4. (a) Dependence of m on α at $\eta = 263$ (crosses) and $\eta = 310$ (triangles); solid lines are obtained by a best fit with Eq. (1). (b) Dependence of m_0^2 on η; the different symbols pertain to different sets of measurements done with either increasing or decreasing n. The solid line is obtained from Eq. (2).

Then, in the range $200 < \eta < 400$, $P(x)$ is very well approximated by

$$P(x) = (Ax^{-\mu} + B)\exp[-m(\alpha,\eta)x], \tag{3}$$

where $m(\alpha,\eta)$ is given by (1) and (2) and μ has the previously determined value. A and B are instead free parameters that can be very easily determined. It is possible to fit our experimental $P(x)$, in the range $0.4\,^\circ\mathrm{C/cm} < \alpha < 3\,^\circ\mathrm{C/cm}$, with $A = 10^5$, $B \simeq 4\times10^3$ for $\eta > \eta_s$, and $B = 0$ for $\eta < \eta_s$. The solid curves in Figs. 3(a) and 3(b) are obtained from Eq. (3).

The feature of $P(x)$ displayed by Eqs. (2) and (3) are typical of phase transitions.[13,14] Therefore, since the transition point η_s is very close to the point where spatiotemporal intermittency sets in, we may conclude that the transition to this behavior is a phase transition.

The main features of $P(x)$ for $\eta \geq \eta_s$ qualitatively agree with those obtained in coupled maps[1a] and PDE[2] in spatiotemporal intermittent regimes. Of course these models do not reproduce the values of the nonuniversal exponents in Eqs. (2) and (3).[1a]

The observation of a power-law decay of $P(x)$ in the range $200 < \eta < \eta_s$ may give useful information for the construction of a phase-transition model[14] for spatiotemporal intermittency. However, below η_s, no detailed theoretical analysis of $P(x)$ performed in coupled maps and PDE's seems to be presently available. Thus to strengthen the reliability of the measured features of $P(x)$ we have also computed the distribution $P(\tau)$ of the laminar regions that last a time τ. We observe that $P(\tau)$ has a functional dependence on τ formally equivalent to Eq. (3). More specifically, below threshold we find in the same range of n an algebraic decay with the same exponent. Furthermore, to verify the influence on the final results of the criteria chosen to distinguish between laminar and turbulent regions, we have performed again the calculation of $P(x)$ using the peak-to-peak amplitude measured on the mean spatial period instead of the temporal one. No appreciable change in the behavior of $P(x)$ has been noticed.

Summarizing, the onset of spatiotemporal intermittency, in Rayleigh-Bénard convection of a medium-Prandtl-number fluid in an annular cell, displays features of a phase transition. Although many aspects of this phenomenon are still to be investigated, the analogy of the behavior of our system with that observed in coupled maps, PDE, and some cellular automata suggests that these models may be very useful to understand the general features of spatiotemporal intermittency.

We are indebted to S. Ruffo and R. Livi for many important suggestions on the study of the phase transition. We also acknowledge useful discussions with F. T. Arecchi, P. Manneville, B. Nicolaenko, A. Politi, and M. A. Rubio and technical assistance from S. Acciai, L. Albavetti, M. D'Uva, and S. Mascalchi. This work has been partially supported by the Gruppo Nazionale di Struttura della Materia (Italy).

[1a]K. Kaneko, Prog. Theor. Phys. **74**, 1033 (1985).

[1b]G. L. Oppo and R. Kapral, Phys. Rev. A **33**, 4219 (1986).

[2]H. Chaté and P. Manneville, Phys. Rev. Lett. **54**, 112 (1987).

[3]J. M. Hyman and B. Nicolaenko, Physica (Amsterdam) **18D**, 113 (1986); B. Nicolaenko, in Proceedings of the International Conference on the Physics of Chaos and Systems Far From Equilibrium, edited by M. Duong-van and B. Nicolaenko, Nucl. Phys. B (to be published).

[4]S. Wolfram, Rev. Mod. Phys. **55**, 601 (1983).

[5]P. Bergé, in Proceedings of the International Conference on the Physics of Chaos and Systems Far From Equilibrium, edited by M. Duong-van and B. Nicolaenko, Nucl. Phys. B (to be published).

[6]M. Van Dyke, *An Album of Fluid Motion* (Parabolic, Stanford, 1982); D. J. Tritton, *Physical Fluid Dynamics* (Van Nostrand, Reinhold, New York, 1979), Chaps. 19–22.

[7]S. Ciliberto, F. Francini, and F. Simonelli, Opt. Commun. **54**, 381 (1985).

[8]S. Ciliberto and M. A. Rubio, Phys. Rev. Lett. **58**, 25 (1987).

[9]This rather strange result observed also by P. Bergé (private communication) should be related with the annular geometry. The number of rolls in all of the experiments, performed in circular and rectangular cells, decreases for increasing ΔT. See, for example, M. Heutmaker and J. Gollub, Phys. Rev. A **35**, 242 (1987). However, numerical simulations done for a two-dimensional flow are consistent with our observations. See J. K. Platten and J. C. Legros, *Convection in Liquids* (Springer-Verlag, New York, 1984), Chap. 6.

[10]The distinction between laminar and turbulent regions solely in terms of the amplitude does not have a rigorous justification. However, this criterion has been used also in theoretical studies (Refs. 1 and 2) because the way of defining the complexity of spatial patterns is still an open problem.

[11]W. Kinzel, Z. Phys. B **58**, 229 (1985).

[12]Y. Pomeau, Physica (Amsterdam) **23D**, 3 (1986).

[13]H. Müller-Krumbhaar, in *Monte Carlo Methods in Statistical Physics*, edited by K. Binder (Springer-Verlag, New York, 1979).

[14]D. R. Nelson, in *Phase Transitions and Critical Phenomena*, edited by C. Domb and J. L. Lebowitz (Academic, London, 1983).